Title

Relationship between Segmental Dynamics Measured by Quasi-Elastic Neutron Scattering and Conductivity in Polymer Electrolytes.

Journal

ACS macro letters, 7(4)

ISSN

2161-1653

Authors

Mongcopa, Katrina Irene S
Tyagi, Madhusudan
Mailoa, Jonathan P
et al.

Publication Date

2018-04-01

DOI

10.1021/acsmacrolett.8b00159

Peer reviewed

ACS Macro Letters

Letter

Cite This: ACS Macro Lett. 2018, 7, 504−508

pubs.acs.org/macroletters

Relationship between Segmental Dynamics Measured by Quasi-Elastic Neutron Scattering and Conductivity in Polymer Electrolytes

Katrina Irene S. Mongcopa,[†] Madhusudan Tyagi,[‡,§] Jonathan P. Mailoa,[∥] Georgy Samsonidze,[∥] Boris Kozinsky,[⊥,∥] Scott A. Mullin,[#] Daniel A. Gribble,[†] Hiroshi Watanabe,[¶] and Nitash P. Balsara*[,†,○,▽]

[†]Department of Chemical and Biomolecular Engineering, University of California, Berkeley, Berkeley, California 94720, United States

[‡]National Institute of Standards and Technology Center for Neutron Research, Gaithersburg, Maryland 20899, United States

[§]Department of Materials Science and Engineering, University of Maryland, College Park, Maryland 20742, United States

[∥]Research and Technology Center, Robert Bosch LLC, Cambridge, Massachusetts 02139, United States

[⊥]John A. Paulson School of Engineering and Applied Sciences, Harvard University, Cambridge, Massachusetts 02138, United States

[#]Seeo Inc., Hayward, California 94545, United States

[¶]Institute for Chemical Research, Kyoto University, Uji, Kyoto 611-0011, Japan

[○]Materials Science Division, Lawrence Berkeley National Laboratory, Berkeley, California 94720, United States

[▽]Joint Center for Energy Storage Research, Lawrence Berkeley National Laboratory, Berkeley, California 94720, United States

Supporting Information

ABSTRACT: Quasi-elastic neutron scattering experiments on mixtures of poly(ethylene oxide) and lithium bis-(trifluoromethane)sulfonimide salt, a standard polymer electrolyte, led to the quantification of the effect of salt on segmental dynamics in the 1−10 Å length scale. The monomeric friction coefficient characterizing segmental dynamics on these length scales increases exponentially with salt concentration. More importantly, we find that this change in monomeric friction alone is responsible for all of the observed nonlinearity in the dependence of ionic conductivity on salt concentration. Our analysis leads to a surprisingly simple relationship between macroscopic ion transport in polymers and dynamics at monomeric length scales.

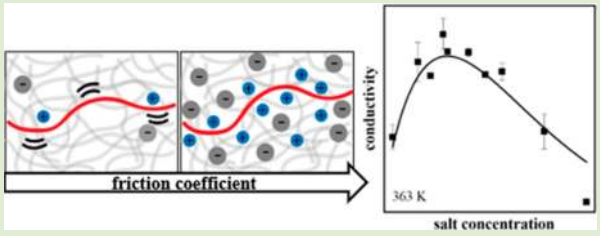

The mechanism of ion conduction in conventional liquid electrolytes, e.g., mixtures of solvents with high dielectric constants such as alkyl carbonates and salts such as $LiPF_6$ used in current lithium-ion batteries, is well established.[1,2] At low salt concentrations, ionic conductivity increases linearly with salt concentration due to an increase in charge carrier concentration. Charge screening, usually modeled using the Debye−Hückel theory,[3] results in deviation from this linear dependence. At high enough concentration, the viscosity of the solution increases significantly, and conductivity decreases with increasing concentration. The dependence of conductivity on salt concentration is thus characterized by a maximum.[4,5]

One approach for improving the performance of rechargeable lithium batteries is to replace the flammable liquid electrolyte with a high molecular weight polymer.[6] The prototypical polymer electrolytes are mixtures of polyethers such as poly(ethylene oxide) (PEO) and lithium bis-(trifluoromethane)sulfonimide (LiTFSI) salt.[7] Similar to the case of liquid electrolytes, conductivity versus salt concentration also exhibits a maximum.[8] However, the conductivity of polymer electrolytes is independent of viscosity; the viscosity of polymers, η, increases sharply with molecular weight, M, as $\eta \sim M^{3.4}$, while ionic conductivity at a fixed salt concentration is independent of M (for $M \geq 4$ kg/mol).[9] Instead, the conductivity of high molecular weight polymers is determined by segmental dynamics which slow down due to associations between polymer chains and salt molecules.[10,11] The purpose of this paper is to clarify the origin of the conductivity maximum observed in polymer electrolytes. In particular, we will address the relative importance of screening and segmental dynamics.

Quasi-elastic neutron scattering (QENS) has emerged as a powerful tool for studying segmental dynamics in polymers.[12−14] The relevant processes occur on length scales between 5 and 50 Å and on time scales between 0.1 and 2 ns. In simple liquids, the mean-square displacement of the constituent molecules, $\langle r^2(t)\rangle$, scales linearly with time, t.[15] In the long chain limit, the mean-square displacement of monomers due to local segmental motion is characterized by $\langle r^2(t)\rangle$ that scales linearly with $t^{1/2}$.[16] In pioneering work, Mao et al. showed that segmental dynamics in amorphous PEO-based electrolytes was slowed down by the addition of salt.[17] More complex behavior is seen in crystalline PEO-based

Received: February 23, 2018
Accepted: April 3, 2018
Published: April 6, 2018

DOI: 10.1021/acsmacrolett.8b00159
ACS Macro Lett. 2018, 7, 504−508

electrolytes,[18] but this is outside the scope of the present study which focuses on amorphous systems.

In this work, we quantify the underlying segmental dynamics at 363 K in polymer electrolytes consisting of PEO (35 kg/mol) and LiTFSI salt concentrations, r_s = 0, 0.08, 0.15, and 0.20 (r_s is the molar ratio of Li^+ to ethylene oxide monomers), and establish the quantitative relationship between segmental dynamics and ionic conductivity. We characterize segmental dynamics measured by QENS using the monomeric friction coefficient, first introduced by Ferry,[19] and show its direct correspondence with ionic conductivity.

Quasi-elastic neutron scattering provides information on the dynamics by measuring the change in energy of the scattered neutrons, $\hbar\omega$.[20] We used the NG2 high-flux backscattering spectrometer (HFBS) at the NIST Center for Neutron Research. Data are collected over time scales ranging from 0.1 to 2 ns and reciprocal space ranging from Q = 0.25 to 1.75 Å^{-1}, where Q is the magnitude of the scattering vector defined as $Q = 4\pi \sin(\theta/2)/\lambda$, where θ is the scattering angle and λ is the nominal wavelength of the incident neutrons. Due to the large incoherent scattering cross section of hydrogen, the scattering intensity is primarily dominated by the incoherent scattering from the polymer backbone. Previous studies have shown that at low Q values ($Q \leq 0.25$ Å^{-1}) the scattering signal from pure PEO has a significant coherent scattering contribution.[21] We thus focus our analysis on $Q > 0.25$ Å^{-1} and correspondingly short time scales.

The dependence of the normalized incoherent structure factor $S_{inc}(Q,\omega)$ on energy, $\hbar\omega$, obtained at a representative scattering vector Q = 0.47 Å^{-1} from these electrolytes is shown in Figure 1a. The instrumental resolution is obtained by measuring the sample at 20 K and appears as a purely elastic signal (solid black line) in the QENS spectra. The decreased width of the structure factor with increasing salt concentration is a signature of the slowing down of segmental dynamics due to associations between polymer segments and salt.

It is convenient to re-express $S_{inc}(Q,\omega)$ in the time domain using a Fourier transform. A program provided by NIST (DAVE[22]) was used to transform the data and account for instrumental resolution. The results are shown in Figure 1b where we plot $S_{inc}(Q,t)/S_{inc}(Q,0)$ as a function of time. It is standard to use a stretched exponential function, or the Kohlrausch–Williams–Watts (KWW) function, to fit the data

$$\frac{S(Q,t)}{S(Q,0)} = \exp\left[-\left(\frac{t}{\tau}\right)^{\beta}\right] \quad (1)$$

where β is the stretched exponential and τ is the relaxation time. The curves in Figure 1b represent KWW fits through the data with β = 0.5 and τ as an adjustable parameter.[23] Note that our measurements do not capture relaxation processes on time scales smaller than 0.1 ns; $S_{inc}(Q,t)/S_{inc}(Q,0)$ does not approach 1 as t approaches 0. Previous studies have shown that these processes are unrelated to segmental relaxation.[24−27] KWW fits are used to analyze data from all the electrolytes in the range Q = 0.37 Å^{-1} to Q = 0.62 Å^{-1}. For completeness, the resulting τ values are given in the Supporting Information.

The average mean-square displacement can be obtained from our measurements using eq 2

$$S_{inc}(Q,t) = \exp\left[\frac{-Q^2}{6}\langle r^2(t)\rangle\right] \quad (2)$$

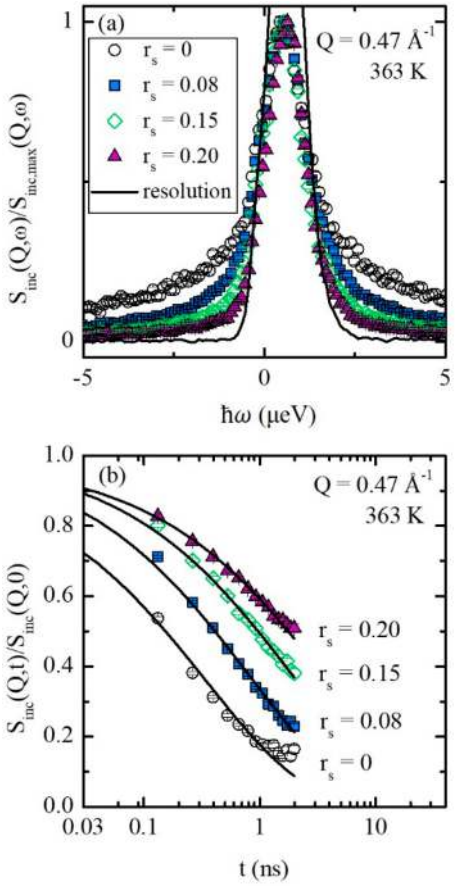

Figure 1. (a) Normalized incoherent structure factor, $S_{inc}(Q,\omega)/S_{inc,max}(Q,\omega)$, in the frequency domain, plotted as a function of energy, $\hbar\omega$, at Q = 0.47 Å^{-1} and 363 K. The structure factor was measured by QENS. (b) Corresponding Fourier transformed data in the time domain. Solid curves represent fits to the KWW function (eq 1).

The dependences of $\langle r^2(t)\rangle$ thus obtained from the electrolytes at a representative value of Q = 0.47 Å^{-1} are shown in Figure 2a. Over most of the available time window, $\langle r^2(t)\rangle$ scales as $t^{1/2}$. This is a standard signature of segmental dynamics.[28,29] In some cases, we found deviations from the expected scaling. In such cases, the fitted range was reduced (e.g., the r_s = 0 data set in Figure 2a). These deviations are due to the proximity of the fast dynamics of neat PEO to the instrumental time resolution and do not affect our fitting parameters. The fitted ranges are given in the Supporting Information.

The solid lines in Figure 2a represent the least-squares fit through the data and are used to determine the Rouse parameter, defined as $p_R = \langle r^2(t)\rangle/t^{1/2}$. In principle, p_R should be independent of Q. Our data are consistent with this expectation, as shown in Figure 2b, where p_R is plotted as a function of Q. The dashed lines in Figure 2b represent the average values of p_R at each salt concentration. The Rouse model, wherein a polymer chain is described in terms of a coarse-grained bead-spring model, yields the following relationship between p_R and the monomeric friction coefficient, ζ[30,31]

$$\zeta = \frac{12k_BTl^2}{p_R^2\pi} \quad (3)$$

DOI: 10.1021/acsmacrolett.8b00159
ACS Macro Lett. 2018, 7, 504−508

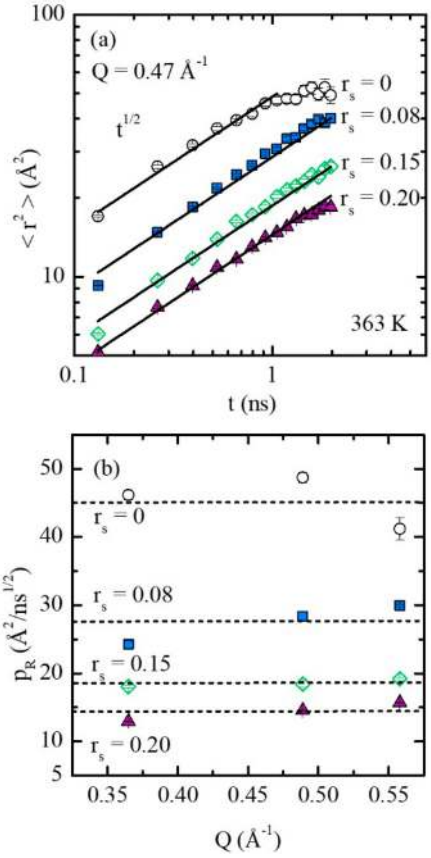

Figure 2. (a) Mean-square displacement, $\langle r^2 \rangle$, as a function of time, t, from QENS experiments at $Q = 0.47$ Å^{-1} with solid lines representing fits to the Rouse scaling, $\langle r^2 \rangle \sim t^{1/2}$. (b) Rouse parameter, p_R, plotted as a function of Q for electrolytes with different salt concentrations, r_s. Dashed lines represent average values of p_R. Error bars represent a 95% confidence interval.

where l is the statistical segment length. Using the known value of l for PEO (5.8 Å),[32] we obtain the dependence of ζ on salt concentration. These results are given in Table 1.

Table 1. Monomeric Friction Coefficient, ζ, from QENS at Different Salt Concentrations

r_s	monomeric friction coefficient, $\zeta \times 10^{-7}$ (g/s)
0	0.32 (±0.06)
0.08	0.87 (±0.20)
0.15	1.87 (±0.12)
0.20	3.16 (±0.63)

One may regard the friction coefficients given in Table 1 as first estimates based on current knowledge of segmental dynamics. The equation used to obtain the coefficients (eq 3) is strictly valid in the context of pure homopolymers only. The presence of salt may alter the relationship between ζ, p_R, and l. Molecular dynamics simulations may shed light on this relationship. In addition, l is likely to change in the presence of salt, due to salt-induced conformational changes.[33] Separate small-angle neutron scattering experiments are required to quantify these effects in the PEO/LiTFSI system.

In Figure 3, we plot the normalized monomeric friction coefficient, $\zeta(r_s)/\zeta(0)$, as a function of salt concentration. It is evident that the monomeric friction coefficient increases

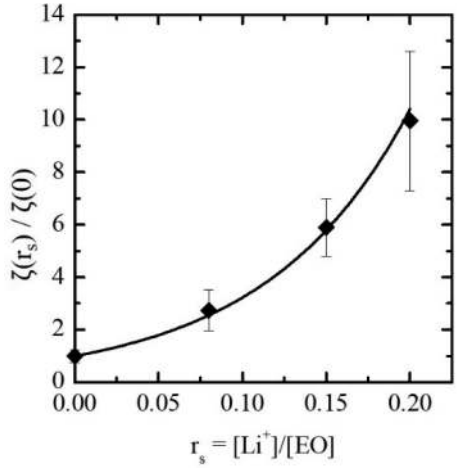

Figure 3. Normalized friction coefficient, $\zeta(r_s)/\zeta(0)$, as a function of salt concentration, r_s. $\zeta(0)$ is the friction coefficient of neat PEO. The solid curve represents eq 4. Error bars represent the standard deviation of the measurements.

exponentially with salt concentration; at $r_s = 0.20$, ζ of the electrolyte is a factor of 10 larger than that of neat PEO. The curve in Figure 3 quantifies the dependence of ζ on r_s according to

$$\frac{\zeta(r_s)}{\zeta(0)} = \exp\left[\frac{r_s}{0.085}\right] \tag{4}$$

where the dimensionless constant 0.085 quantifies the exponential slowing of segmental relaxation due to the presence of salt in PEO/LiTFSI at 363 K. The values of ζ determined from p_R ($= \langle r^2(t) \rangle / t^{1/2}$) reflect the friction experienced by a coarse-grained Rouse segment, and both glassy and rubbery relaxation processes contribute to this ζ.[49] Experimental data indicate that at temperatures well above the glass transition temperature (true for systems examined in this study) the friction coefficients associated with these two processes exhibit similar temperature dependencies.[49] Thus, at fixed temperatures, the ratio $\zeta(r_s)/\zeta(0)$ can be utilized to quantify the effect of salt on segmental dynamics.

In Figure 4, we plot the conductivity of the electrolytes, measured by ac impedance spectroscopy, as a function of salt concentration. The data exhibit a maximum in the vicinity of $r_s = 0.08$, consistent with the literature.[8,34,35] The curve in Figure 4 represents eq 5

$$\sigma = 0.043 r_s \left[\exp\left(-\frac{r_s}{0.085}\right)\right] \text{S/cm} \tag{5}$$

where we have combined the expected effects of increasing r_s: a linear increase in charge carrier concentration and slowing of segmental dynamics measured by QENS. The prefactor, 0.043 S/cm, is the specific conductivity of dilute PEO/LiTFSI electrolytes (with the electrolyte concentration, r_s, being a dimensionless quantity). To our knowledge, eq 5 represents the first attempt to quantify, on a purely experimental basis, the relationship between ionic conductivity and segmental relaxation. It is evident in Figure 4 that the data are consistent with the proposed relationship. The wide concentration range over which our result is valid is noteworthy; eq 5 applies to PEO/LiTFSI electrolytes with salt concentrations ranging from 0 up to 4.5 molal. While this expression applies to data at 363

DOI: 10.1021/acsmacrolett.8b00159
ACS Macro Lett. 2018, 7, 504−508

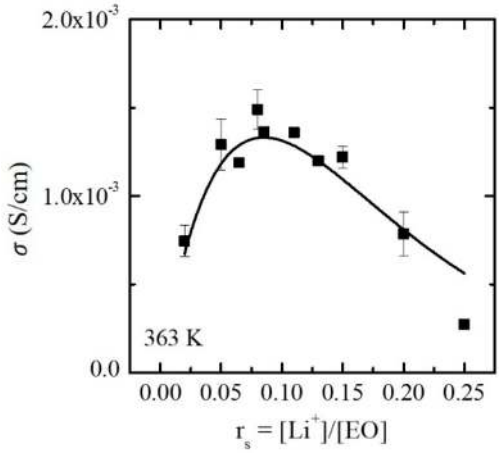

Figure 4. Conductivity, σ, measured at 363 K from ac impedance spectroscopy plotted as a function of salt concentration, r_s. The solid curve represents eq 5. Error bars represent the standard deviation of the measurements.

K, we expect the same form to apply at other temperatures in which the conductive media forms a single phase.

The reported dependence of conductivity on salt concentration in Figure 4 is consistent with the vast literature on PEO/LiTFSI mixtures.[8,9,36,37] Likewise, our QENS data are also consistent with previous studies.[27,38−40] The main advance is that we conducted ac impedance and QENS on the same polymer samples and sought to relate results from these separate experiments. While many have noted the correlation between ion transport and segmental motion,[8,41−43] the direct connection between conductivity and monomeric friction that eq 5 embodies has not been recognized.

It is important to realize that eq 5 is not a fit through the conductivity data. The agreement between eq 5 and the data in Figure 4 indicates that all of the nonlinearity of the dependence of conductivity on salt concentration can be explained by monomeric friction coefficients measured independently by QENS. In other words, the slowing of ion transport of both Li^+ and $TFSI^-$ ions due to salt-polymer interactions is accurately reflected in the motion of hydrogen atoms on the polymer backbone. Deviations from the linear scaling of conductivity with salt concentration thus do not arise due to charge screening, as is the case in conventional liquid electrolytes.[44]

In summary, we have used QENS to quantify the effect of salt on segmental dynamics in a standard polymer electrolyte, PEO/LiTFSI. The Rouse model was used to determine the effect of salt addition on the monomeric friction coefficient. The deviation from linearity of the dependence of ionic conductivity on salt concentration is quantitatively consistent with changes in the monomeric friction coefficient determined by QENS. While the importance of segmental dynamics in polymer electrolytes has been noted by many,[39,40,45−48] we are not aware of any previous study that suggests that it is the *only* effect that is responsible for the nonlinear dependence of conductivity on salt concentration. Ion transport in binary electrolytes such as PEO/LiTFSI is characterized by three transport coefficients: conductivity, salt diffusion coefficient, and the transference number. Our work thus far only addresses the effect of monomeric friction coefficient on conductivity. In a future work, we will study the effect of the monomeric friction coefficient on the other two transport properties.

■ ASSOCIATED CONTENT

Supporting Information

The Supporting Information is available free of charge on the ACS Publications website at DOI: 10.1021/acsmacrolett.8b00159.

Experimental section, KWW fit parameters, and mean-square displacement as a function of time at other Q values and errors (PDF)

■ AUTHOR INFORMATION

Corresponding Author

*E-mail: nbalsara@berkeley.edu.

ORCID

Katrina Irene S. Mongcopa: 0000-0001-5393-6871

Nitash P. Balsara: 0000-0002-0106-5565

Notes

The authors declare no competing financial interest.

■ ACKNOWLEDGMENTS

This work was supported by the Bosch Energy Research Network grant. Access to the HFBS was provided by the Center for High Resolution Neutron Scattering, a partnership between the National Institute of Standards and Technology and the National Science Foundation under Agreement No. DMR-1508249.

■ REFERENCES

(1) Newman, J.; Thomas-Alyea, K. E. *Electrochemical Systems*, 3rd ed.; John Wiley & Sons, Inc.: NJ, 2004.

(2) Robinson, R. A.; Stokes, R. H. *Electrolyte Solutions*, 2nd Revised ed.; Dover Publications, Inc., 2002.

(3) Hückel, E.; Debye, P. Zur Theorie der Elektrolyte. I. Gefrierpunktserniedrigung und verwandte Erscheinungen. *Phys. Z.* **1923**, *24*, 185−206.

(4) Kraus, C. A. Electrolytes: from dilute solutions to fused salts. *J. Phys. Chem.* **1954**, *58*, 673−683.

(5) Pitzer, K. S. Electrolytes. from dilute solutions to fused salts. *J. Am. Chem. Soc.* **1980**, *102*, 2902−2906.

(6) Goodenough, J. B.; Kim, Y. Challenges for rechargeable Li batteries. *Chem. Mater.* **2010**, *22*, 587−603.

(7) Scrosati, B.; Vincent, C. A. Polymer electrolytes: the key to lithium polymer batteries. *MRS Bull.* **2000**, *25*, 28−30.

(8) Lascaud, S.; Perrier, M.; Vallée, A.; Besner, S.; Prud'homme, J.; Armand, M. Phase diagrams and conductivity behavior of poly-(ethylene oxide)-molten salt rubbery electrolytes. *Macromolecules* **1994**, *27*, 7469−7477.

(9) Teran, A. A.; Tang, M. H.; Mullin, S. A.; Balsara, N. P. Effect of molecular weight on conductivity of polymer electrolytes. *Solid State Ionics* **2011**, *203*, 18−21.

(10) Bruce, P. G.; Vincent, C. A. Polymer electrolytes. *J. Chem. Soc., Faraday Trans.* **1993**, *89*, 3187−3203.

(11) Borodin, O.; Smith, G. D. Mechanism of ion transport in amorphous poly(ethylene oxide)/ LiTFSI from molecular dynamics simulations. *Macromolecules* **2006**, *39*, 1620−1629.

(12) Richter, D.; Ewen, B. Neutron spin-echo investigations on the dynamics of polymers. *J. Appl. Crystallogr.* **1988**, *21*, 715−728.

(13) Zorn, R.; Arbe, A.; Colmenero, J.; Frick, B.; Richter, D.; Buchenau, U. Neutron scattering study of the picosecond dynamics of polybutadiene and polyisoprene. *Phys. Rev. E: Stat. Phys., Plasmas, Fluids, Relat. Interdiscip. Top.* **1995**, *52*, 781−795.

(14) Bée, M. Localized and long-range diffusion in condensed matter: State of the art of QENS studies and future prospects. *Chem. Phys.* **2003**, *292*, 121−141.

(15) Hansen, J. P.; McDonald, I. R. Theory of simple liquids. In *Theory of Simple Liquids*, 3rd ed.; Elsevier. 2006.

DOI: 10.1021/acsmacrolett.8b00159
ACS Macro Lett. 2018, 7, 504−508

(16) Kimmich, R. *Principles of Soft-Matter Dynamics: Basic Theories, Non-Invasive Methods, Mesoscopic Aspects*; Springer: New York, 2012; p 430.
(17) Mao, G. M.; Saboungi, M. L.; Price, D. L.; Armand, M.; Mezei, F.; Pouget, S. Alpha-relaxation in PEO-LiTFSI polymer electrolytes. *Macromolecules* **2002**, *35*, 415−419.
(18) Fullerton-Shirey, S. K.; Maranas, J. K. Effect of LiClO4 on the structure and mobility of PEO-based solid polymer electrolytes. *Macromolecules* **2009**, *42*, 2142−2156.
(19) Ferry, J. D.; Landel, R. F. Molecular friction coefficients in polymers and their temperature dependence. *Colloid Polym. Sci.* **1956**, *148*, 1−6.
(20) Jobic, H.; Renouprez, A.; Bée, M.; Poinsignon, C. Quasi-elastic neutron scattering. *J. Phys. Chem.* **1986**, *90*, 1059−1065.
(21) Senses, E.; Tyagi, M.; Natarajan, B.; Narayanan, S.; Faraone, A. Chain dynamics and nanoparticle motion in attractive polymer nanocomposites subjected to large deformations. *Soft Matter* **2017**, *13*, 7922−7929.
(22) Azuah, R. T.; Kneller, L. R.; Qiu, Y.; Tregenna-Piggott, P. L.; Brown, C. M.; Copley, J. R.; Dimeo, R. M. DAVE: A comprehensive software suite for the reduction, visualization, and analysis of low energy neutron spectroscopic data. *J. Res. Natl. Inst. Stand. Technol.* **2009**, *114*, 341−358.
(23) Richter, D.; Monkenbusch, M.; Arbe, A.; Colmenero, J. *Neutron spin echo in polymer systems. Adv. Polym. Sci.*; Springer: Berlin, 2005; Vol.*174*, pp 1−221.
(24) Mao, G.; Perea, R. F.; Howells, W. S.; Price, D. L.; Saboungi, M. L. Relaxation in polymer electrolytes on the nanosecond timescale. *Nature* **2000**, *405*, 163−165.
(25) Saboungi, M. L.; Price, D. L.; Mao, G.; Fernandez-Perea, R.; Borodin, O.; Smith, G. D.; Armand, A.; Howells, W. S. Coherent neutron scattering from PEO and a PEO-based polymer electrolyte. *Solid State Ionics* **2002**, *147*, 225−236.
(26) Tyagi, M.; Arbe, A.; Alvarez, F.; Colmenero, J. Short-range order and collective dynamics of poly(vinyl acetate): A combined study by neutron scattering and molecular dynamics simulations. *J. Chem. Phys.* **2008**, *129*, 1−14.
(27) Do, C.; Lunkenheimer, P.; Diddens, D.; Götz, M.; Weib, M.; Loidl, A.; Sun, X. G.; Allgaier, J.; Ohl, M. Li+ transport in poly(ethylene oxide) based electrolytes: Neutron scattering, dielectric spectroscopy, and molecular dynamics simulations. *Phys. Rev. Lett.* **2013**, *111*, 1−5.
(28) Niedzwiedz, K.; Wischnewski, A.; Monkenbusch, M.; Richter, D.; Genix, A. C.; Arbe, A.; Colmenero, J.; Strauch, M.; Straube, E. Polymer chain dynamics in a random environment: Heterogeneous mobilities. *Phys. Rev. Lett.* **2007**, *98*, 1−4.
(29) Brodeck, M.; Alvarez, F.; Arbe, A.; Juranyi, F.; Unruh, T.; Holderer, O.; Colmenero, J.; Richter, D. Study of the dynamics of poly(ethylene oxide) by combining molecular dynamic simulations and neutron scattering experiments. *J. Chem. Phys.* **2009**, *130*, 1−13.
(30) Rouse, P. E. A Theory of the linear viscoelastic properties of dilute solutions of coiling polymers. *J. Chem. Phys.* **1953**, *21*, 1272−1273.
(31) Doi, M. *Introduction to Polymer Physics*; Oxford University Press, Inc.: New York, 1996; Vol. *21*, p 107.
(32) Niedzwiedz, K.; Wischnewski, A.; Allgaier, J.; Richter, D. Chain dynamics and viscoelastic properties of poly(ethylene oxide). *Macromolecules* **2008**, *41*, 4866−4872.
(33) Borodin, O.; Smith, G. Molecular dynamics simulations of poly(ethylene oxide)/LiI melts. 1. structural and conformational properties. *Macromolecules* **1998**, *31*, 8396−8406.
(34) van Zon, A.; de Leeuw, S. W. A Rouse model for polymer electrolytes. *Electrochim. Acta* **2001**, *46*, 1539−1544.
(35) Pesko, D. M.; Timachova, K.; Bhattacharya, R.; Smith, M. C.; Villaluenga, I.; Newman, J.; Balsara, N. Negative transference numbers in poly(ethylene oxide)-based electrolytes. *J. Electrochem. Soc.* **2017**, *164*, E3569−E3575.
(36) Devaux, D.; Bouchet, R.; Glé, D.; Denoyel, R. Mechanism of ion transport in PEO/LiTFSI complexes: Effect of temperature, molecular weight and end groups. *Solid State Ionics* **2012**, *227*, 119−127.
(37) Huynh, T. V.; Messinger, R. J.; Sarou-Kanian, V.; Fayon, F.; Bouchet, R.; Deschamps, M. Restricted lithium ion dynamics in PEO-based block copolymer electrolytes measured by high-field nuclear magnetic resonance relaxation. *J. Chem. Phys.* **2017**, *147*, 134902−1−134902−8.
(38) Mos, B.; Verkerk, P.; Pouget, S.; van Zon, A.; Bel, G. J.; de Leeuw, S. W.; Eisenbach, C. D. The dynamics in polyethyleneoxide-alkali iodide complexes investigated by neutron spin-echo spectroscopy and molecular dynamics simulations. *J. Chem. Phys.* **2000**, *113*, 4−7.
(39) Triolo, A.; Arrighi, V.; Triolo, R.; Passerini, S.; Mastragostino, M.; Lechner, R. E.; Ferguson, R.; Borodin, O.; Smith, G. D. Dynamic heterogeneity in polymer electrolytes. Comparison between QENS data and MD simulations. *Phys. B* **2001**, *301*, 163−167.
(40) Triolo, A.; Lo Celso, F.; Passerini, S.; Arrighi, V.; Lechner, R. E.; Frick, B.; Triolo, R. Segmental dynamics in polymer electrolytes. *Appl. Phys. A: Mater. Sci. Process.* **2002**, *74*, S493−S495.
(41) Druger, S. D.; Ratner, M. A.; Nitzan, A. Generalized hopping model for frequency-dependent transport in a dynamically disordered medium, with applications to polymer solid electrolytes. *Phys. Rev. B: Condens. Matter Mater. Phys.* **1985**, *31*, 3939−3947.
(42) Ratner, M. A.; Johansson, P.; Shriver, D. F. Polymer electrolytes: ionic transport mechanisms and relaxation coupling. *MRS Bull.* **2000**, *25*, 31−37.
(43) Webb, M. A.; Jung, Y.; Pesko, D. M.; Savoie, B. M.; Yamamoto, U.; Coates, G.; Balsara, N.; Wang, Z. G.; Miller, T. F. Systematic computational and experimental investigation of lithium-ion transport mechanisms in polyester-based polymer electrolytes. *ACS Cent. Sci.* **2015**, *1*, 198−205.
(44) Fisher, M. E.; Levin, Y. Criticality in ionic fluids: Debye-Hückel theory, Bjerrum, and beyond. *Phys. Rev. Lett.* **1993**, *71*, 3826−3829.
(45) Rey, I.; Lassègues, J. C.; Grondin, J.; Servant, L. Infrared and raman study of the PEO-LiTFSI polymer electrolyte. *Electrochim. Acta* **1998**, *43*, 1505−1510.
(46) Georén, P.; Lindbergh, G. Characterisation and modelling of the transport properties in lithium battery polymer electrolytes. *Electrochim. Acta* **2001**, *47*, 577−587.
(47) Russina, O.; Triolo, A.; Aihara, Y.; Telling, M. T. F.; Grimm, H. Quasi-elastic neutron scattering investigation of dynamics in polymer electrolytes. *Macromolecules* **2004**, *37*, 8653−8660.
(48) Maitra, A.; Heuer, A. Understanding segmental dynamics in polymer electrolytes: A computer study. *Macromol. Chem. Phys.* **2007**, *208*, 2215−2221.
(49) Inoue, T.; Osaki, K. Role of polymer chain flexibility on the viscoelasticity of amorphous polymers around the glass transition zone. *Macromolecules* **1996**, *29*, 1595−1599.

DOI: 10.1021/acsmacrolett.8b00159
ACS Macro Lett. 2018, 7, 504−508